Since January 2020 Elsevier has created a COVID-19 resource centre with free information in English and Mandarin on the novel coronavirus COVID-19. The COVID-19 resource centre is hosted on Elsevier Connect, the company's public news and information website.

Atmospheric Pollution Research 12 (2021) 101172

Contents lists available at ScienceDirect

Atmospheric Pollution Research

journal homepage: www.elsevier.com/locate/apr

Global assessment of tropospheric and ground air pollutants and its correlation with COVID-19

H.R. Naqvi [a,*], G. Mutreja [b], M. Hashim [a], A. Singh [a], M. Nawazuzzoha [a], D.F. Naqvi [c], M. A. Siddiqui [a], A. Shakeel [a], A.A. Chaudhary [d], A.R. Naqvi [e]

[a] Department of Geography, Faculty of Natural Sciences, Jamia Millia Islamia, New Delhi, India
[b] Environmental Systems Research Institute, R & D Center, New Delhi, India
[c] ZiMetrics Technologies Pvt. Ltd., Pune, India
[d] Department of Biology, College of Science, Imam Mohammad Ibn Saud Islamic University, Riyadh, 13317-7544, Saudi Arabia
[e] Department of Periodontics, College of Dentistry, University of Illinois at Chicago, Chicago, IL, USA

ARTICLE INFO

Keywords:
COVID-19
Pandemic lockdown
Tropospheric pollutants
Air quality
Mortality

ABSTRACT

The declaration of COVID-19 pandemic by the WHO initiated a series of lockdowns globally that varied in stringency and duration; however, the spatiotemporal effects of these lockdowns on air quality remain understudied. This study evaluates the global impact of lockdowns on air pollutants using tropospheric and ground-level indicators over a five-month period. Moreover, the relationship between air pollution and COVID-19 cases and mortalities was examined. Changes in the global tropospheric (NO_2, aerosols, and O_3) and ground-level ($PM_{2.5}$, PM_{10}, NO_2, and O_3) pollutants were observed, and the maximum air quality improvement was observed immediately after lockdown. Except for a few countries, a decline in air pollutants correlated with a reduction in Land Surface Temperature (LST). Notably, regions with higher tropospheric NO_2 and aerosol concentrations were also COVID-19 hotspots. Our analysis showed moderate positive correlation for NO_2 with COVID-19 cases ($R^2 = 0.33$; $r = 0.57$, $P = 0.006$) and mortalities ($R^2 = 0.40$; $r = 0.63$, $P = 0.015$), while O_3 showed a weak-moderate positive correlation with COVID-19 cases ($R^2 = 0.22$; $r = 0.47$, $P = 0.003$) and mortalities ($R^2 = 0.12$; $r = 0.35$, $P = 0.012$). However, $PM_{2.5}$, and PM_{10} showed no significant correlation with either COVID-19 cases or mortality. This study reveals that humans living under adverse air pollution conditions are at higher risk of COVID-19 infection and mortality.

1. Introduction

In December 2019, Severe Acute Respiratory Syndrome Coronavirus 2 (SARS-CoV-2) was identified in Wuhan, China, which was associated with a pneumonia-like illness termed Coronavirus Disease-19 (COVID-19). The virus spread rapidly worldwide, and by the end of January 2020, the World Health Organization (WHO) declared COVID-19 a pandemic (Huang et al., 2020; Cucinotta and Vanelli, 2020), which initiated a series of lockdowns in various countries commencing in Wuhan, China on January 23, 2020, and subsequently imposed by Italy (March 10), Spain (March 14), France (March 18), India (March 25), Iran (March 28), and globally by April (Sicard et al., 2020). Depending on the severity of transmission in different countries, lockdown required partial or complete containment of public interactions, leading to a halt in anthropogenic activities.

Daily pollutant emissions from industries, traffic, and the energy production sectors significantly contribute to poor air quality and adversely affect human health and quality of life. According to a 2014 WHO report, one out of every eight deaths worldwide is attributed to air pollution amounting to 4.9 million deaths per year (WHO, 2014). According to a 2017 study, O_3 and $PM_{2.5}$ caused 0.5 million and 3 million deaths, respectively, globally (State of Global Air, 2019). It was predicted that maintaining $PM_{2.5}$ concentrations based on the WHO guidelines would likely increase the life expectancy in 11 of the most populated countries.

The evaluation of environmental pollutants during the COVID-19 lockdown revealed variations (increase or reduction) in the levels of NO_2, PM, CO, O_3, and other APs, indicating that a temporary pause in

Peer review under responsibility of Turkish National Committee for Air Pollution Research and Control.
* Corresponding author.
E-mail address: hnaqvi1@jmi.ac.in (H.R. Naqvi).

https://doi.org/10.1016/j.apr.2021.101172
Received 15 March 2021; Received in revised form 13 August 2021; Accepted 15 August 2021
Available online 17 August 2021

human activities can restore air quality within a few months (Sicard et al., 2020; Nakada and Urban, 2020), and the improved air quality was correlated with a decline in air pollution-related deaths during the lockdown period (Dutheil et al., 2020). Interestingly, the relationship between air pollution and cases/mortalities related to SARS-CoV-2 further highlights that exposure to environmental pollutants may exacerbate the clinical manifestation of COVID-19 (Zhu et al., 2020; Conticini et al., 2020). People residing in polluted regions are more prone to viral infection and may succumb to illnesses due to a weakened immune system, primarily caused by the inhalation of toxic APs (including $PM_{2.5}$, $PM_{10}$and NO_2) (Viehmann et al., 2015; Schraufnagel et al., 2019). Solimini et al. showed a positive association of exposure to air-borne particulate matter ($PM_{2.5}$ and PM_{10}) with COVID-19 cases and indicated that a slight increase in these pollutant indicators may exacerbate disease severity (Solimini et al., 2021). Another study also revealed a direct relationship between the concentration of $PM_{2.5}$ and COVID-19 mortality using machine-learning analysis (Mele and Magazzino, 2020). Multiple studies have shown a significant positive correlation of NO_2 and $PM_{2.5}$with COVID-19 cases and mortalities and considered them dominant environmental factors responsible for adverse outcomes (Zhu et al., 2020; Yao et al., 2020; Konstantinoudis et al., 2020; Ogen, 2020; Pansini and Fornacca, 2020). Previous short-term studies have examined the correlation between the COVID-19 lockdowns and air quality restoration at a national and regional levels (Shrestha et al., 2020; Urrego and Urrego, 2020); however, only limited studies have examined the global assessment of tropospheric and ground-level APs during the COVID-19 pandemic and the correlation between COVID-19 cases/mortalities and ground-level pollutant levels.

In this study, we systematically and comprehensively evaluated spatiotemporal changes in multiple tropospheric (NO_2, aerosols, and O_3) and ground-level ($PM_{2.5}$, PM_{10}, NO_2, and O_3) pollutants from January–May 2020 (post-lockdown) and compared them with the corresponding months in 2019 (pre-lockdown). Our findings explicitly show a correlation between the COVID-19 lockdown and global improvement in air pollution levels and provide a strong evidence that higher pollutant concentrations in densely populated areas disproportionately predispose humans to COVID-19-associated mortalities.

2. Materials and methods

2.1. Data assimilation for the global assessment of air pollution parameters

Remote sensing data were analyzed utilizing the Google Earth Engine platform, which enabled the geospatial analysis (Gorelick et al., 2017). NO_2 and O_3 data were collected from the Copernicus Sentinel-5 Precursor Tropospheric Monitoring Instrument, which is widely utilized for air quality applications (Veefkind et al., 2012) and is beneficial for monitoring daily NO_2 concentrations (Tobías et al., 2020). MCD19A2.006: Terra and Aqua MAIAC Land Aerosol Optical Depth (AOD) Daily 1-km global datasets were obtained through the United States Geological Survey portal (USGS: https://lpdaac.usgs.gov/products/mcd19a2v006/), and the values were visualized (upscaled) from 0 to 1000 and utilized to determine the variations in atmospheric aerosols. For Land Surface Temperature (LST) analysis and spatial variation, MOD11A1.006 Terra LST and Emissivity Daily Global 1-km data products (Wan et al., 2015) were utilized. A global spatiotemporal analysis was performed for January–May 2019 and 2020. The COVID-19 lockdowns drastically influenced the air pollutants level; therefore, the daily average NO_2, O_3, and AOD values (January–May) were extracted and converted to monthly average values for 12 major countries (Brazil, Canada, China, France, Germany, India, Iran, Italy, Russia, Spain, the UK, and the USA), which were (and remain) COVID-19 hotspots. Moreover, the impact of air quality on radiant emissivity was assessed utilizing LST data for the same period, and detailed analyses were performed for multiple countries.

Average daily ground pollutant data of more than 40 major locations worldwide, obtained from the World-wide Air Quality Monitoring Data Coverage website (https://aqicn.org/sources/), were utilized to analyze monthly average changes in air pollutants (January–May 2019 and 2020) using ground-level $PM_{2.5}$, PM_{10}, NO_2, and O_3 concentrations (Fu et al., 2020; Hashim et al., 2021; Kumari and Toshniwal, 2020; Liu et al., 2021). To assure that the air pollutant changes were caused by the COVID-19 lockdowns in 2020, we compared data from Berlin, Cardiff, Delhi, Istanbul, Madrid, Milan, Moscow, Mumbai, New York City, Paris, Quebec, Sao Paulo, and Wuhan for the corresponding period in 2019, due to their data availability. The percent change for all the APs was calculated and represented graphically for each country and city.

2.2. COVID-19 mortality and AP correlation/regression analysis

Pearson's correlation and linear regression analyses were performed to assess the relationship between COVID-19 cases/mortalities with the four ground-level APs ($PM_{2.5}$, PM_{10}, NO_2, and O_3). We used strong, moderate and poor correlation criteria defined by Ratner (2009). Based on this, correlation coefficient values between 0 and 0.3 indicate a weak positive linear relationship, between 0.3 and 0.7 indicate a moderate positive linear relationship and between 0.7 and 1.0 indicate a strong positive linear relationship. The COVID-19 cases and mortality data are available by country, but very few places have available data at the city level (Coronavirus COVID-19 Live Tracker Johns Hopkins; https://www.grainmart.in/news/coronavirus-covd-19-live-cases-tracker-john-hopkins/). Based on the data availability, we selected 20–22 cities for correlation analysis. After initial findings, we removed multiple outliers that might have skewed the results. For final analysis, 15–17 cities were selected (Berlin, Cardiff, Castello, Hualqui, Limburg, Madrid, Boston, Milan, Moscow, Mumbai, Jersey City, New York City, Rome, Stockholm, Ventanas, and Wuhan) for which COVID-19 cases/mortalities and *in situ* ground-level air quality indicator data were available. These locations represent major COVID-19 hotspots with >5000 reported COVID-19 cases as of June 22, 2020. For consistency of our COVID-19 datasets, we did not account for the lag times due to the SARS-CoV-2 incubation period (generally considered as 15 days).

3. Results

3.1. Marked reduction in the tropospheric NO_2 density

Global reductions in tropospheric NO_2 concentrations were observed post-lockdown compared with pre-lockdown concentrations (Fig. 1 and fig. S1). The NO_2 column density concentrations are indicated by cyan and red patches for concentrations ranging from 0.00001 to 0.0001 mol/m^2. In January 2020, the concentration of red and yellow patches was high over Asia (China, India, Iran, and Iraq), Europe (Germany, Italy, Poland, UK, and France), North America (USA and Canada), Russia, and some equatorial African nations (Fig. 1, a and fig. S1, a). The earliest indication of the impact of the lockdowns on the NO_2 levels occurred in China, where the concentration reduced from 0.0001 to 0.00005 mol/m^2 (January to February 2020, respectively), and the concentration of red patches diminished. Compared to the corresponding months in 2019, no apparent changes were observed for the rest of the regions except Germany and Poland (Fig. 1, b and fig. S1, b). The immediate improvement in NO_2 levels that occurred post-lockdown was evident as pollutant concentrations decreased over most countries. Notably, in March, an increase in red patches was observed over China and generally remained the same until April 2020 compared with the corresponding 2019 data (Fig. 1c and d, and fig. S1, c and d). NO_2 concentrations declined to <0.00005 mol/m^2 by the end of May in most countries (Fig. 1e and fig. S1, e).

To assess the lockdown impact on tropospheric NO_2 concentrations, monthly averages (January–May 2020) were obtained for 12 major

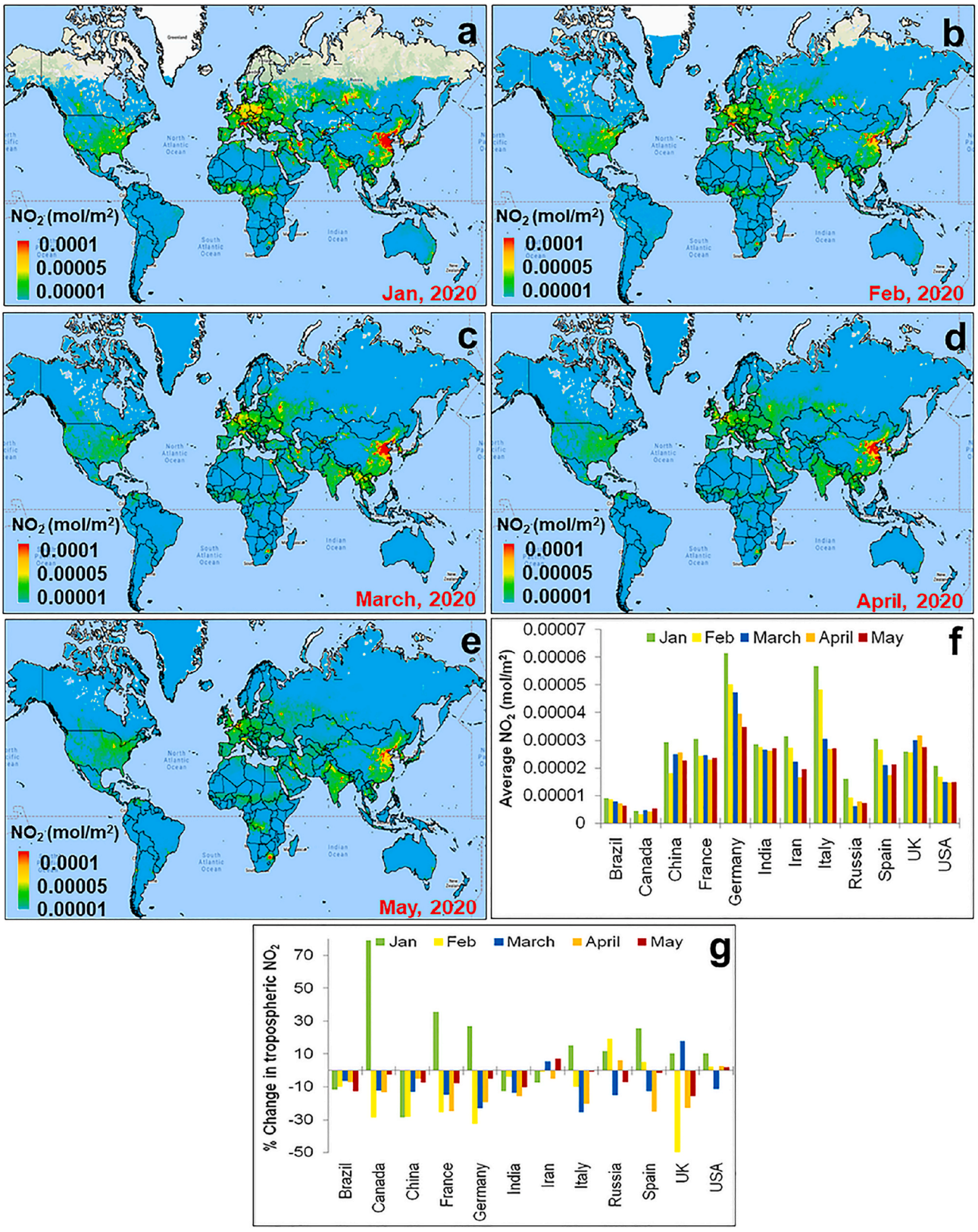

Fig. 1. COVID-19 lockdown impact on tropospheric NO_2 in 2020. Map showing global satellite-derived average NO_2 concentrations in (**a**) January, (**b**) February, (**c**) March, (**d**) April, and (**e**) May. A gradual decline in global tropospheric NO_2 is evident in most regions, as observed by the reduction in red patches. (**f**) Histograms showing the average tropospheric NO_2 concentration (mol/m^2) variations in 12 countries (representing Asia, Europe, and North and South America) with high COVID-19 cases as of June 22, 2020. (**g**) Percentage change in tropospheric NO_2 of selected countries for January–May 2020 compared to the corresponding period in 2019. The quantitative reduction in tropospheric NO_2 corroborates with the qualitative decline determined by the global spatial variations map.

COVID-19 hotspot countries (Fig. 1f), and then, the percentage change from January–May 2019 was calculated. The major variation in the reduction percentage values in most of the countries was observed in the post-lockdown months. The overall average (January–May) values were considered to also cover partial and temporary lockdown durations. The most prominent impacts on NO_2 were observed in China and India, with average reductions of 28.39% and 15.9%, respectively, in the first months of lockdown (Fig. 1g and Table S1). European countries benefited from the lockdowns during the study period. The overall average NO_2 concentrations (mol/m^2) were high in the UK (3.516E-05), Germany (5.398E-05), Italy (4.098E-05), and France (2.811E-05) from January–May 2019 (Table S1), and this study calculated average decreases of 10.60%, 8.19%, 7.47%, and 1.79% in the UK, Germany, Italy, and France, respectively (Fig. 1g). In both periods, the average NO_2 concentrations were higher in Italy and Germany than in the rest of the countries (Fig. 1f and fig. S1, f). These regions are industrialized and highly populated, which are known major NO_2 emission contributors in Italy (Leibniz Institute for Tropospheric Research (TROPOS), 2020), resulting in higher pollutant concentrations in these countries. Iran (0.13%) and Spain (1.79%) exhibited the smallest NO_2 reductions; however, a drastic cyclic pattern for the NO_2 concentrations was observed in the USA and Russia, which decreased in March, increased in April, and decreased again in May (Fig. 1g and Table S1).

3.2. Global variations in aerosols under COVID-19 lockdown

Aerosol optical depth (AOD) is a quantitative estimate of aerosols (scaled up values) within a column of air from the surface of the earth to the top of the atmosphere. These aerosols are generated by human activities such as vehicular and industrial emissions, dust particles generated in mining, and urban smog. The COVID-19 lockdown resulted in the shutdown of all economic activities, curbing aerosol emissions. The AOD maps for January–May 2019 and 2020 show the global patterns and reductions in the aerosol concentrations (Fig. 2a–e, and fig. S2, a toe). Compared with 2019, the concentration and spread of the blue patches, which represent lower AOD values, are evident in 2020. Generally, the AOD values, represented by yellow-red patches, were high (scaled up values 700–1000) in China, India, and the west-central African nations. These concentrations remained stable in India, exhibited a reasonable decline in eastern China, and increased in west-central Africa and southeast Australia in February 2020 (Fig. 2a and b). The AOD values almost vanished over these regions by the end of March 2020 (Fig. 2c), whereas the AOD values in these regions increased in March 2019 compared to January–February 2019 and the corresponding period in 2020 (fig. S2, a–c).

New epicenters of high aerosol density were observed in Vietnam, Thailand, Peru, and Cambodia. In China, the aerosols over the central-eastern region shifted toward the southeast, which further increased in April 2020 (Fig. 2, d and fig. S2, d). The AOD values improved drastically in the aforementioned countries in the Northern Hemisphere, whereas the intensity remained similar in the Southern Hemisphere in May 2020 compared to those of January–April 2020 and 2019 (Fig. 2, e and fig. S2, e). These variations in the different countries are evident in the histograms for January–May 2019 compared with those of the lockdown period of January–May 2020 (Fig. 2, f and fig. S2, f).

Next, an AOD values percentage change analysis was performed for 12 countries representing Asia, Europe, and North and South America. In China, Russia, Canada, and the USA, average AOD values were higher in all the lockdown months except May compared to the corresponding 2019 concentrations due to the unavailability of satellite datasets in the extreme Northern Hemisphere nations. Considering this drawback in extracting the average AOD values that may have influenced the output, our visual interpretation of China indicates that, the extent of high aerosol concentrations represented by red patches reduced in February 2020 (post-lockdown). Unlike the other countries where abrupt changes in the AOD occurred during lockdown, stable AOD values were observed in Brazil, with an average reduction of 10.69% during the study period (Fig. 2, g and Table S1). Overall average reductions (January–May 2020) were observed in Russia (7.48%), Canada (5.79%), and the UK (2.49%) (Fig. 2, g and Table S1). In May, reduction in AOD values were observed in the USA (22.6%), Italy (22.8%), and Canada (41.5%). Interestingly, the overall average AOD values increased in Spain (39.22%) and China (13.24%) but reduced in the post-lockdown months. However, in the rest of the studied countries, the average AOD values increased by 6%, particularly in India, where the AOD values was high in February due to seasonal crop residue fires in the northern states (Punjab, Haryana, and Western Uttar Pradesh).

3.3. Restoration of tropospheric ozone concentration post-lockdown

Compared to 2019, we observed significant changes (generally reduction) in the tropospheric O3 concentrations during the study period (Fig. 3a–e), highlighting the beneficial outcome of the lockdown. The O_3 concentrations were similar from January–May 2019. O_3 concentrations ranging from 0.15 to 0.2 mol/m^2 were observed in the Northern Hemisphere countries, particularly above the $23^{1/2}$ North latitudes, whereas lower concentrations (0.1–0.15 mol/m^2) were reported in the Southern Hemisphere. The O_3 concentrations were comparatively high in these regions in the corresponding months of 2019 (fig. S3, a–e). In January 2020, the concentrations of the red and yellow patches (0.15–0.2 mol/m^2) were greater in Canada, the USA, Russia, and northern China, which consistently increased until February 2020 (Fig. 3a and b). However, in February, the concentration increased in Canada, whereas minimal concentrations were observed in eastern Russia. Although the O_3 concentrations were high during the corresponding 2019 periods, they can be compared utilizing the concentration of the red patches (fig. S3, a and b). The O_3 concentrations began increasing over Europe (France, Germany, Poland, and Italy) in March 2020; however, they reduced over North America, drastically increased over Russia, and gradually increased in India, Australia, Africa, and South America, as evidenced by the conversion of the dark blue patches to cyan at the end of March 2020. This pattern was similar during the corresponding months in 2019; however, the intensity of the changes was greater in 2020 than in 2019 (Fig. 3, c and fig. S3, c). In April 2020, the tropospheric O_3 concentrations over both hemispheres were extremely minimal and incomparable except for the drastic increase over North America. Minimal improvement was observed over Europe and northern China (Fig. 3, d and fig. S3, d). Tropospheric O_3 column concentrations showed global reduction in 2020, whereas its concentrations and their intensities (notice the color-coded spectrum) were high throughout the corresponding months in 2019 (Fig. 3, e and fig. S3, e).

The O_3 concentrations, patterns, and variations in each month were similar, whereas the spatial coverage of the concentrations and their intensities were different (Fig. 3, f and fig. S3, f). In 2019, the five-month average tropospheric O_3 concentrations (mol/m^2) were highest in Russia (0.190), Canada (0.182), and Germany (0.160), and the lowest concentrations were observed in Brazil (0.115) and India (0.117). In 2020, these average O_3 concentrations declined in Canada (0.172), Russia (0.165), and the USA (0.158), leading to O_3 pollution (Table S1). It was observed that in Russia, Canada, and Brazil, the O_3 concentrations reduced monthly; India was the only country where the concentrations increased every month, and the rest of the countries had decreased concentrations mainly in April and May (Fig. 3, g).

3.4. Spatiotemporal changes in global land surface temperature (LST)

Aerosols, believed to have a critical impact on LST, reduce the LST in two ways. First, they cause a reduction in surface isolation by absorbing and scattering. Second, sulfate aerosols found in abundance over industrial regions have a cooling effect (Freychet et al., 2019; Jin et al., 2010; Steiner et al., 2013; Huang et al., 2006). Comparison of the LST

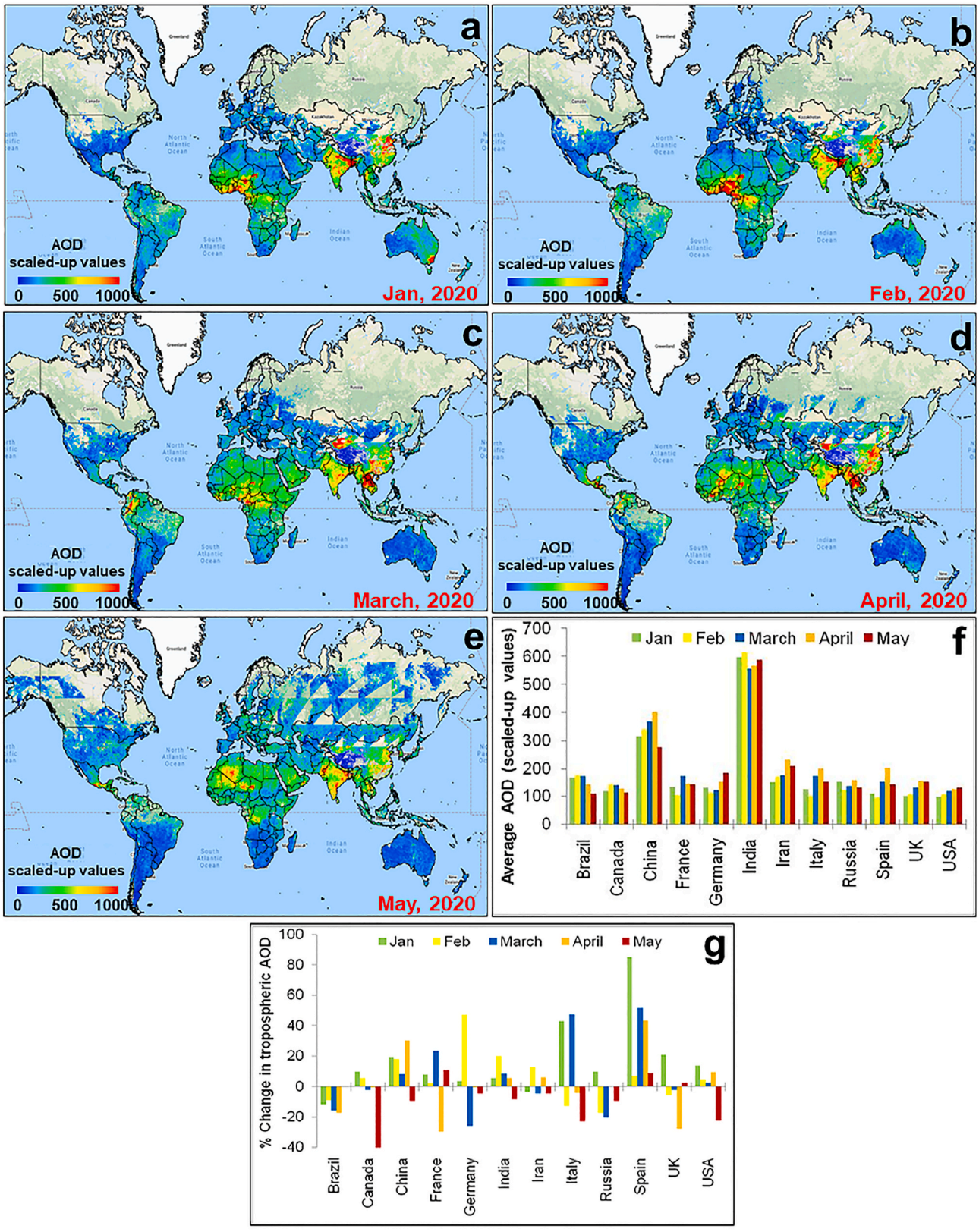

Fig. 2. Pre- and post-lockdown tropospheric aerosol concentrations worldwide. Global atmospheric aerosol optical density (AOD) data were procured, and the scaled-up values (from 0 to 1000) were mapped for (**a**) January, (**b**) February, (**c**) March, (**d**) April, and (**e**) May 2020. A marked decline is evident in China, India, West Africa, Australia, and Brazil. Compared to those in January 2020, the red/yellow patches denoting high AOD values changed to green/blue by May 2020, indicating AOD reductions. (**f**) Histograms showing average AOD values variations in 12 countries. (**g**) Percentage change in tropospheric AOD values in 12 countries from January–May 2020 compared to the corresponding period in 2019.

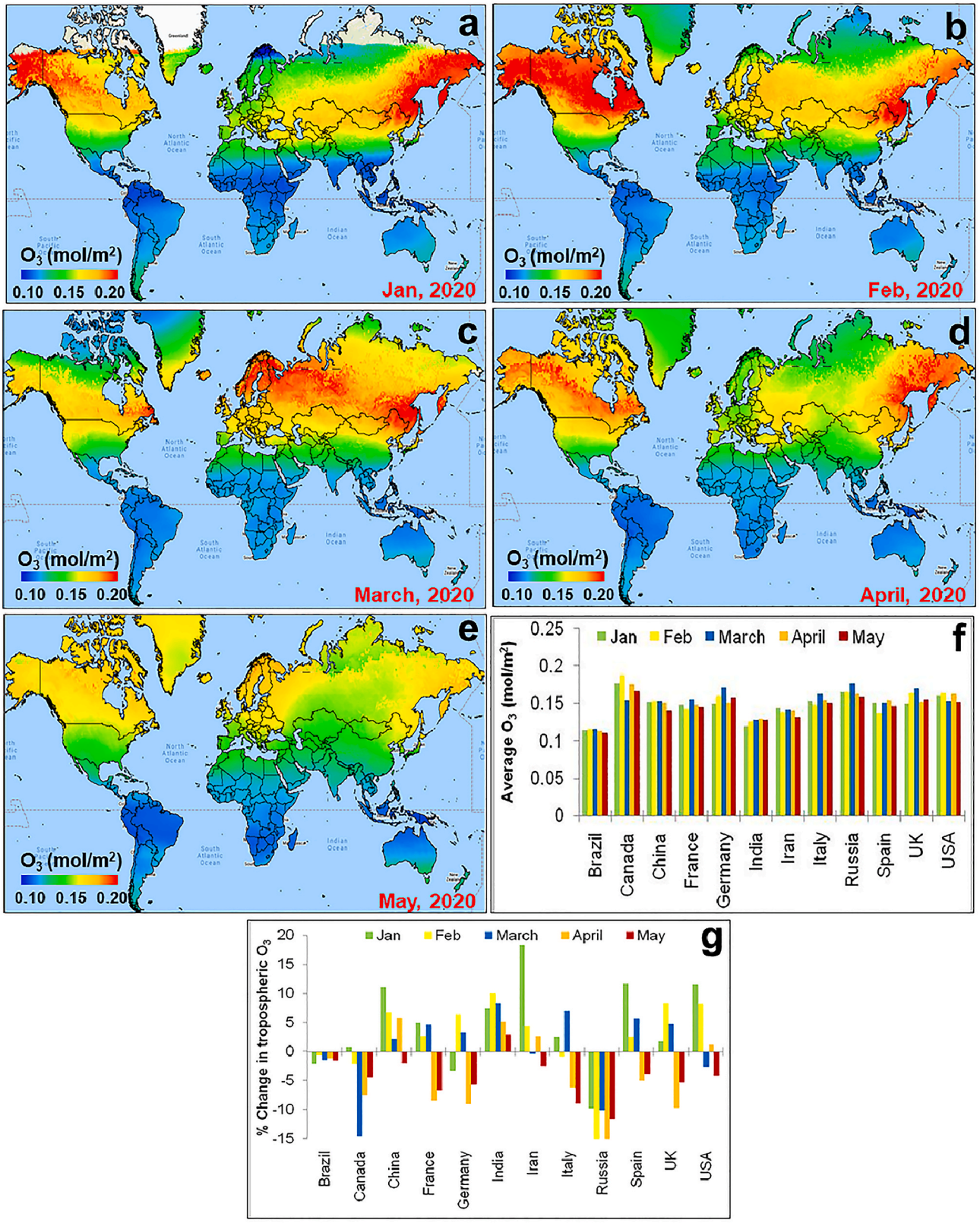

Fig. 3. Spatiotemporal changes in O_3 concentrations in 2020. World map showing O_3 spatial variations in (**a**) January, (**b**) February, (**c**) March, (**d**) April, and (**e**) May. (**f**) Histograms for 12 selected countries showing monthly average O_3 concentrations (mol/m^2). (**g**) Percentage change in O_3 concentrations for the 12 selected countries from January–May 2020 compared to the corresponding period in 2019.

maps for January–May of 2019 and 2020 revealed that the LST has increased over the Northern Hemisphere (LST range of 25–50 °C). Moreover, the variation in LSTs (0–25 °C) and pixel transformation from green to yellow indicates the increased changes in the Northern Hemisphere. However, decreasing trends were observed in the Southern Hemisphere as the intensity of red patches was suppressed gradually over time due to the shifting of the location of the sun (Fig. 4a–e, and fig. S4, a to e). This is attributed to summer onset in the Northern Hemisphere, particularly between the equator and the Tropic of Cancer. Similar increasing LST patterns were observed from temperate to Polar Regions where the color patches steadily changed from blue to green (LST values of −50 to 0 °C). The changes were opposite in the Southern Hemisphere (Fig. 4a–e, and fig. S4, a to e).

The histograms show a similar pattern for 2019 and 2020, and the average LST indicates that the values increased continuously from January to May in 2019 and 2020 for all 12 studied countries (Fig. 4, f and fig. S4, f). The examination of the 2020 global LST maps shows increasing (five-month average) trends in various countries, such as China (14%), Italy (15%), and France (15%), compared to the 2019 LST maps, whereas reductions were observed in these countries in March. The remaining countries (Iran, the UK, Canada, and the USA) showed an LST increase of up to 4%. A higher reduction percentage throughout the period was observed in tropical and temperate nations such as India (4.74%), Brazil (1.59%), and Spain (3.42%). A similar observation was observed in Russia, which is under sub-polar climate conditions (Fig. 4, g) and has a large geographical area that could have influenced the average LST. In Canada, the LST primarily increased in March (27%) and April (19%); however, a marked decrease (29%) occurred in May (Table S1), which is attributed to a sudden increase in the AOD. Brazil, with no imposed lockdown, showed a consistent decline in LST percentage change from January–May 2020, and the LST changes were minimal. Fluctuations from January–May 2020 were observed in the USA due to the partial lockdowns enforced in different areas of the country (Fig. 4, g).

Only India showed a consistent decrease in the LST percentage change among the studied countries because a strict countrywide lockdown was enforced until the end of May 2020. These findings indicate that an LST decrease correlates with a concomitant reduction in ground-level air quality (including PM), tropospheric NO_2 density, and improved O_3 concentration post-lockdown. A comparison of the April 2020 AOD values and LST percentage change showed that a negative change in AOD values correlates with a positive change in LST and vice versa (Fig. 3, g and Fig. 4, g), suggesting that the reduction in aerosols is linked to an increase in the LST during the lockdown in 2020.

3.5. Ground-level air pollutant levels in major locations worldwide

Global satellite datasets do not yield accurate ground-level pollutant concentrations, which have a significant impact on human health. Therefore, in this study, ground-level air pollutant data of $PM_{2.5}$, PM_{10}, NO_2, and O_3 (μg/m^3) were collected, based on availability, for more than 40 locations worldwide to assess patterns and post-lockdown trends. The locations selected represent the countries included in the tropospheric pollutant comparison analysis. The monthly average $PM_{2.5}$ and PM_{10} concentrations were highest in Asia (Delhi, Mumbai, Kolkata, Dhaka, Wuhan, Istanbul, Tehran, Dubai, and Singapore), followed by Europe (Milan, Rome, Paris, Berlin, Madrid, Zurich, Saint Petersburg, and Offange), North America (New York City, Jersey City, Boston, Merced Mexico, Metepec Toluca, and Quebec), and South America (Sao Paulo, Carapungo Quito, and Ventanas) (Fig. 5a and b).

An apparent reduction in PM was observed in Indian cities (Delhi, Mumbai, and Kolkata), which had two-fold higher PM concentrations than the rest of the studied locations. The overall average $PM_{2.5}$ and PM_{10} concentrations were highest in Mumbai (227 μg/m^3 for both), Delhi (198 and 230 μg/m^3, respectively), and Kolkata (150 and 147 μg/m^3, respectively) (Table S2). In these cities, PM concentrations were apparently highest in January and February, declined in March, and further decreased in April and May 2020 (Fig. 5a and b) during the COVID-19 lockdown. A similar trend was observed for NO_2, which showed minimal concentrations by the end of May 2020. The average NO_2 concentrations (μg/m^3) were highest in Tehran (41.62), Delhi (34.23), and Istanbul (33.03), followed by Ankara, Paris, and Zurich, and the lowest NO_2 concentrations mainly occurred in March 2020 in these areas (Fig. 5, c and Table S2). This could be primarily attributed to the traffic restrictions in these locations during the lockdown. However, the O_3 concentrations were low until February and increased in April and May 2020 (Fig. 5c and d), which is the opposite pattern to the NO_2, $PM_{2.5}$, and PM_{10} concentration patterns. The monthly average O_3 concentrations (μg/m^3) from January–May 2020 were highest in Santana (79.51), Stockholm (65.38), Bray (65.21), and Delhi (56.47), and decreased sharply after the lockdown was initiated in March (Fig. 5, d and Table S2).

The average monthly data of 11 cities corroborates with the tropospheric air pollutants obtained from the satellite data. Comparative analysis of the 2019 and 2020 data showed reductions (>20% in most places) in $PM_{2.5}$ and PM_{10} in all the investigated cities, except for Milan and Madrid (Fig. 6a and b). The spatial distribution, direction, and magnitude of PM changes near the surface are substantially different from those of the tropospheric aerosols assessed via satellite data, indicating the significance of monitoring ground-level changes in air pollution compared to satellite-retrieved global patterns and trends. The lockdown impact provided up to a 50% reduction in PM in Madrid, Milan, Moscow, and Mumbai (Fig. 6, c). The O_3 concentration percent change increased (>30%) in most cities but was reduced in Madrid and Sao Paulo across all months. Interestingly, Delhi recorded a continuous increase in the O_3 concentration throughout the study period and saw a maximum increase (up to 120%) in April and May (Fig. 6, d).

3.6. Correlation analysis of COVID-19 cases/mortalities and APs

This study attempted to determine whether humans in regions with high AP concentrations are more vulnerable to COVID-19 infection/mortality and which APs are predominantly associated with COVID-19. To evaluate this, data was obtained from 15 cities including Berlin, Cardiff, Castello, Hualqui, Limburg, Madrid, Boston, Milan, Moscow, Mumbai, Jersey City, New York City, Rome, Stockholm, Ventanas, and Wuhan, representing Asia, Europe, and North and South America. These locations were selected based on the availability of both the required data and having a minimum of 5000 COVID-19 cases as of June 22, 2020. New York City had the highest number of cases (213,056) and mortalities (22,343), followed by Milan, Wuhan, and Madrid, whereas the lowest number of cases (<10,000) and mortalities (<215) were reported in Hualqui, Berlin, and Moscow (Fig. 7a and b).

A linear regression and correlation analysis of the COVID-19 cases and mortalities with the NO_2, $PM_{2.5}$, PM_{10}, and O_3 concentrations was performed for the aforementioned locations. Depending on the pollutant data availability, we initially performed analysis including 20–22 cities globally. However, we did not notice any correlation values for $PM_{2.5}$ (fig. S5, a and b), PM_{10} (fig. S5, c and d) or O_3 (fig. S5, g and h) due to outliers except NO_2 (for cases- $R^2 = 0.06$; $r = 0.24$; for mortalities- $R^2 = 0.07$; $r = 0.28$) and (fig. S5, e and f). For subsequent analysis, we therefore removed 5–6 outliers to obtain more reproducible results. Accordingly, our analysis showed highest correlation between NO_2 and COVID-19 cases ($R^2 = 0.33$; $r = 0.57$, $P = 0.006$) or mortalities ($R^2 = 0.40$; $r = 0.63$, $P = 0.015$) (Fig. 7c and d). O_3 showed a weak-moderate positive correlation with COVID-19 cases ($R^2 = 0.22$; $r = 0.47$, $P = 0.003$) and mortalities ($R^2 = 0.12$; $r = 0.35$, $P = 0.012$) (Fig. 7e and f), while PM_{10} and $PM_{2.5}$ showed no association with COVID-19 cases ($R^2 = 0.08$ and 0.001; $r = -0.29$ and -0.03, respectively) or mortalities ($R^2 = 0.071$ and 0.028; $r = -0.31$ and 0.16), respectively (fig. S6, a to d). These results evidently show that higher pollutant (particularly NO_2 and O_3) levels likely exacerbate COVID-19 infection and mortality. Overall,

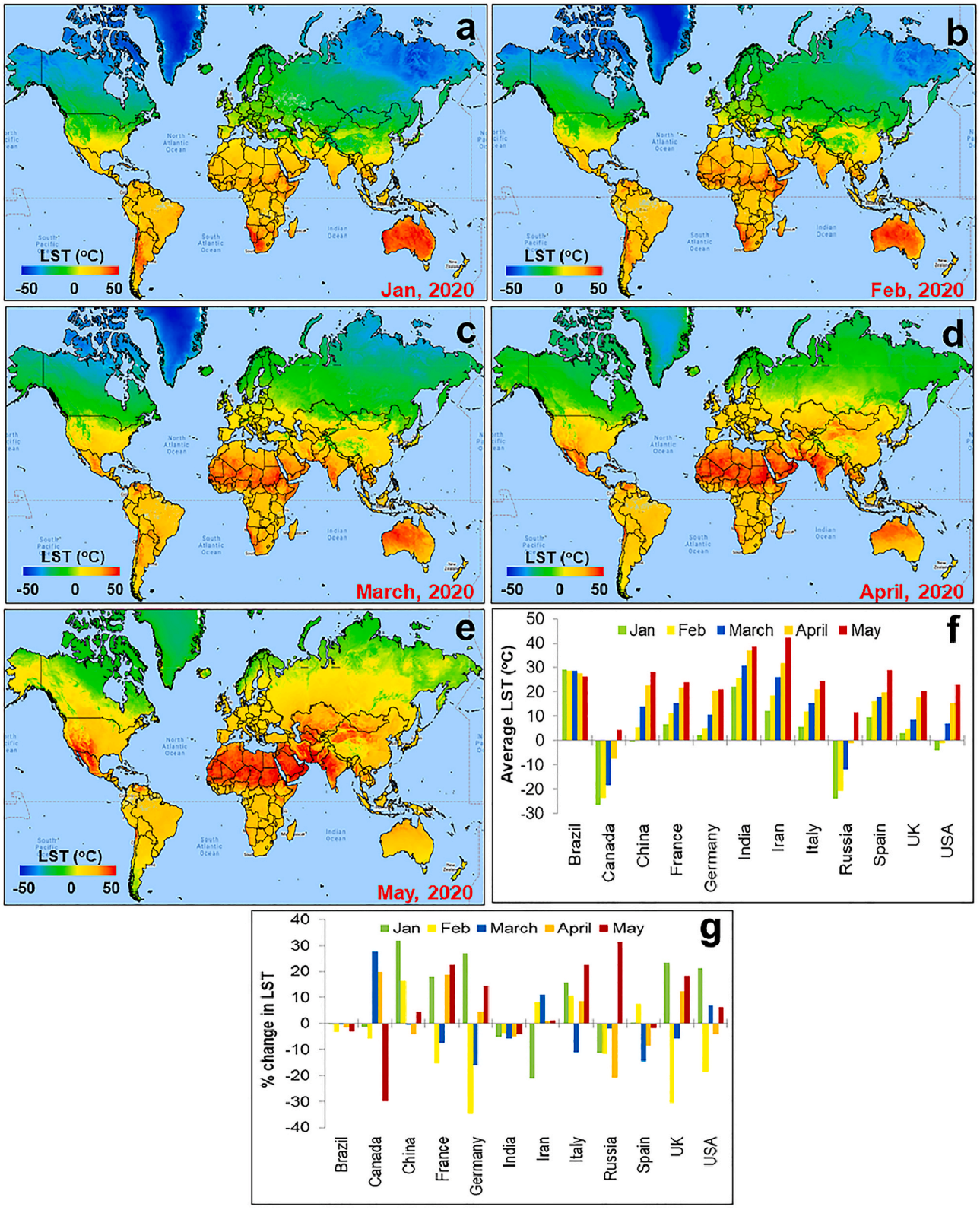

Fig. 4. 2020 Land surface temperatures (LSTs). World map showing average LSTs (in °C) in (**a**) January, (**b**) February, (**c**) March, (**d**) April, and (**e**) May. The intensity of red patches increases over the Northern Hemisphere and decreases in the Southern Hemisphere. (**f**) Histograms showing LST variations in 12 selected countries. LST has a direct relationship with solar radiation, and the analyzed countries were primarily located in the Northern Hemisphere. The graphs show increasing trends from January–May 2020, except in Brazil, which is located at the equator. (**g**) LST percentage changes show a marked decline in most of the studied countries.

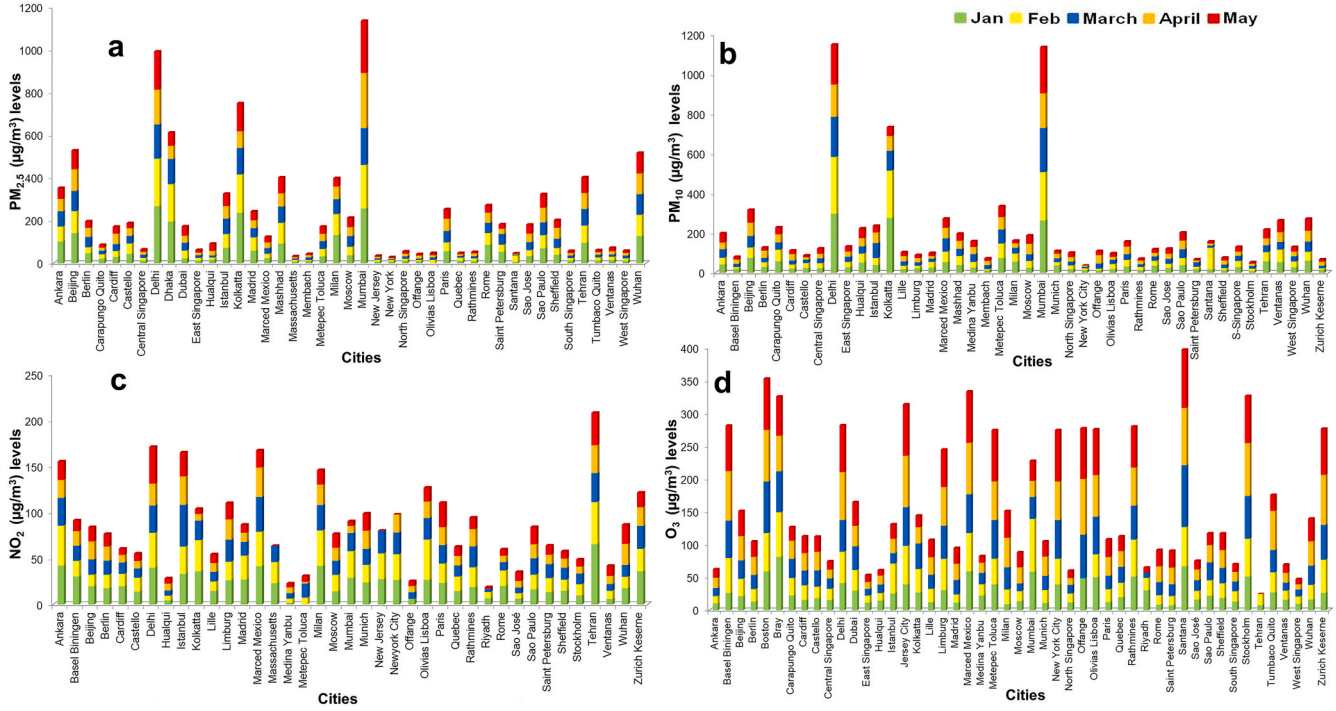

Fig. 5. Ground-level air pollutant concentrations in major locations worldwide. Stacked bars showing monthly average (January–May 2020) (**a**) $PM_{2.5}$, (**b**) PM_{10}, (**c**) NO_2, and (**d**) O_3 concentrations (µg/m^3) in 45 highly populated COVID-19 hotspot locations. Asian cities had the highest $PM_{2.5}$ and PM_{10} concentrations, and most of the locations had high NO_2 and O_3 concentrations.

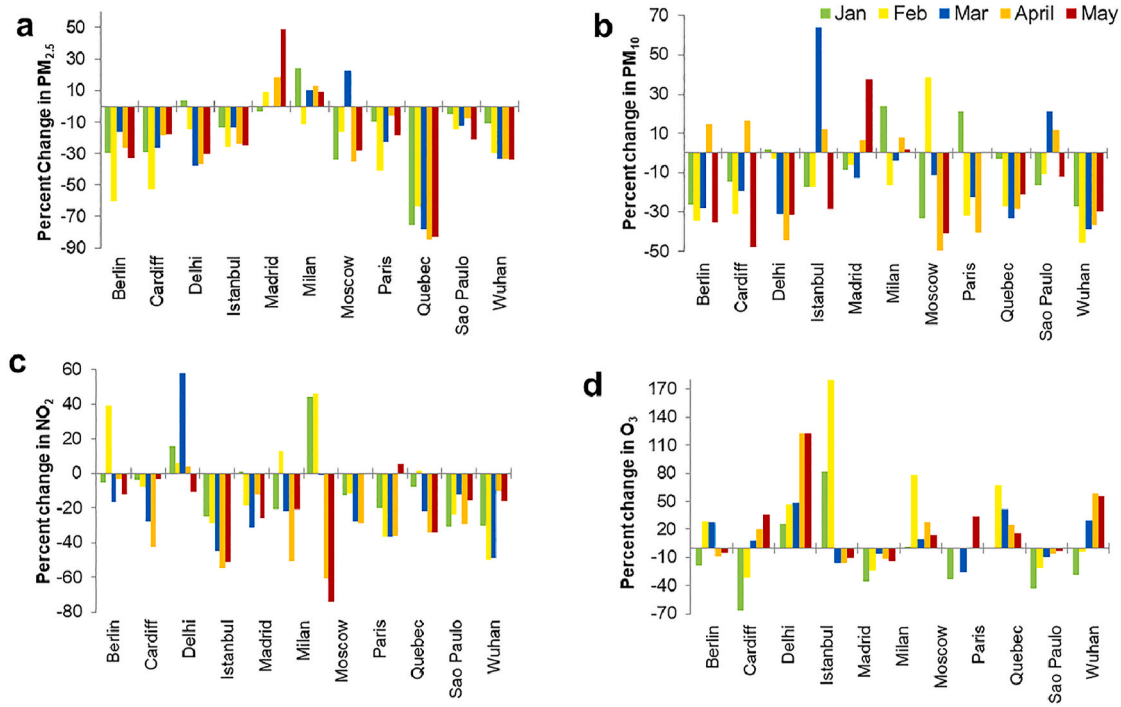

Fig. 6. Reduction in the ground-level air pollutants in metropolitan cities. Percentage change in the ground-level (**a**) $PM_{2.5}$, (**b**) PM_{10}, (**c**) NO_2, and (**d**) O_3 concentrations (µg/m^3) in 11 major metropolitan cities for which both 2019 and 2020 air quality monitoring data was available. Monthly concentration averages from January–May 2020 were compared to the corresponding period in 2019.

both ground-level and tropospheric pollutants can be utilized to predict the adverse outcomes of COVID-19 infection and mortality.

4. Discussion

In this study, a five-month (January–May 2019 and 2020) comprehensive analysis of global tropospheric and ground-level AP indicators was performed to assess the impact of the COVID-19 lockdowns. This

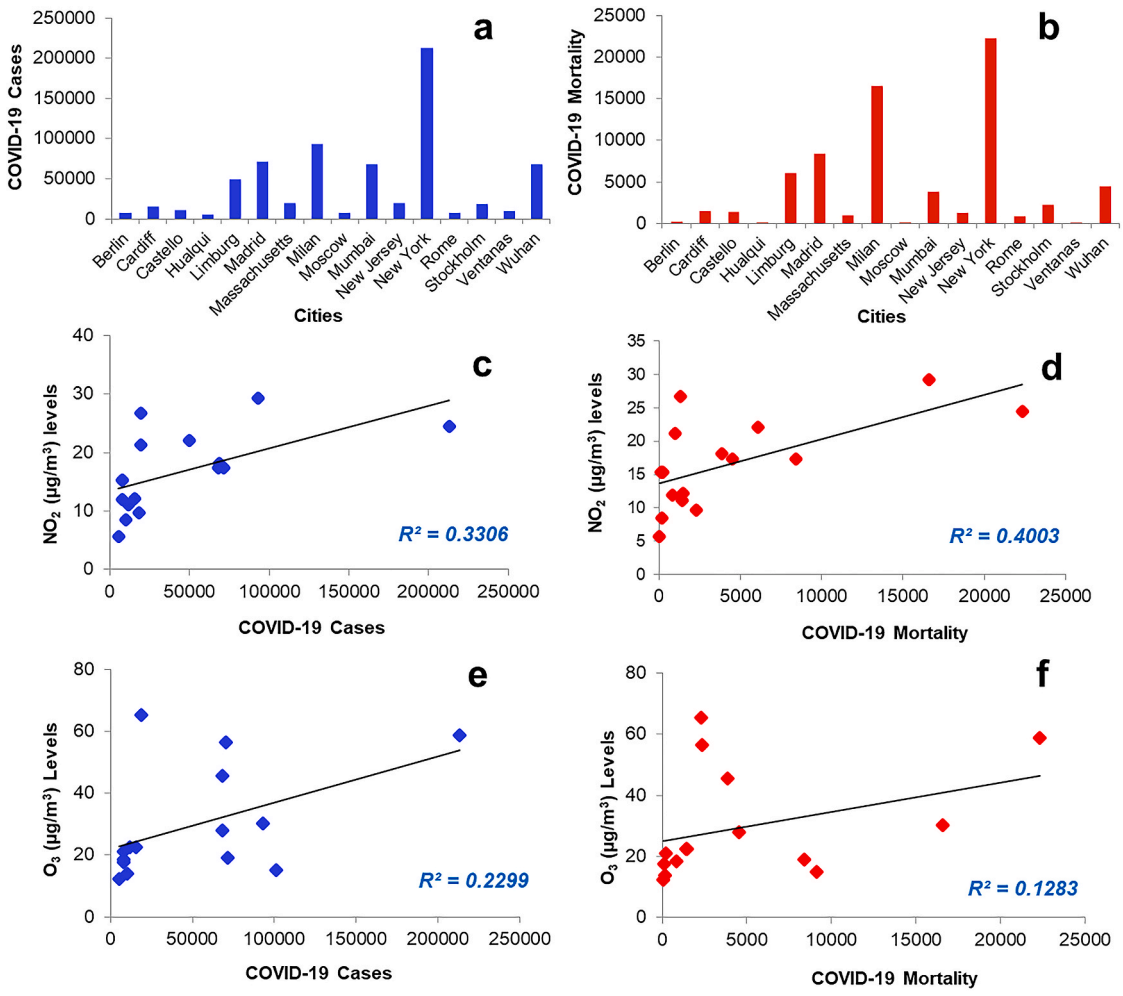

Fig. 7. Correlation analysis of NO_2 and O_3 with COVID-19 cases and mortality. Histograms showing COVID-19 (**a**) cases and (**b**) mortalities in 15 highly populated locations. These locations were selected based on the availability of ground-level AP and COVID-19 cases/mortalities data. Only locations with >5000 COVID-19 cases (as of June 22, 2020) were considered for this analysis. The linear regression analysis results of COVID-19 cases and mortalities with (**c** and **d**) NO_2 (µg/m^3) and (**e** and **f**) O_3, respectively.

analysis is unique from previous reports that performed ground-level and tropospheric pollutant analyses only between January–March 2020 (Venter et al., 2020) because during the January–March 2020 period, most countries had not yet imposed or had only recently imposed a COVID-19 lockdown. In this systematic, unbiased, and long-term analysis, we assessed global AP levels during pre- and post-lockdown periods and correlated the association between APs and COVID-19 cases/mortalities. The results revealed a drastic reduction in tropospheric NO_2 and AOD and ground-level $PM_{2.5}$, PM_{10}, and NO_2. Interestingly, the ground-level NO_2 and O_3, respectively, showed moderate (0.3–0.7) and weak-moderate (0.1–0.5) positive correlation with both COVID-19 cases and mortality. Our findings unequivocally demonstrate that the COVID-19 lockdowns improved global air pollution and identify specific pollutants as the predictors of the adverse outcomes of COVID-19.

A decline in tropospheric NO_2 concentrations was observed immediately post-lockdown, and these concentrations were maintained throughout the study period. The calculated average (January–May) NO_2 concentrations showed that major reductions occurred in Asian countries such as China and India. Previous studies reported similar observations that showed a 30% NO_2 reduction over Chinese cities (Dutheil et al., 2020; NASA, 2020). The average reduction determined by this study was 11.24%, which agrees with previous studies that determined NO_2 reductions of <12% post-lockdown over India (Biswal et al., 2020; Naqvi et al., 2020; Singh and Chauhan, 2020). In the urban regions of Brazil, a 54.3% post-lockdown reduction in $NO_2$was previously reported, supporting the results of this study (Nakada and Urban, 2020). Marked improvement in NO_2 concentrations (~30% decrease) were recorded post-lockdown in Europe (Spain, Italy, and France) and the UK (ESA , 2020; Gautam, 2020).

For most of the countries investigated in this study, a reduction in the AOD was primarily observed in April and May 2020, suggesting that the length of time required assessing atmospheric levels is greater than the time required to assess tropospheric NO_2 levels. This is because aerosols, unlike other pollutants, do not settle. Accordingly, the AOD results in this study showed a major reduction in May 2020 compared to May 2019 in most of the investigated countries. Similar trends in AOD reduction were reported in a recent study that conducted a global analysis of APs post-lockdown (Venter et al., 2020). Additionally, several regional studies have documented AOD reductions in their findings, which support the results of this study. The AOD index score of >0.9 over eastern China until February 2020 was reduced compared to the corresponding period in 2019 (Fan et al., 2020). The National Aeronautics and Space Administration reported that aerosol concentrations recorded in India during the lockdown were the lowest in the past 20 years (Huang et al., 2006). In the European countries, the AOD values decrease also portrayed similar findings to previous studies that showed decrease in aerosol concentration over urban and rural regions

(Menut, 2020). European AOD values in March 2020 were influenced by dry weather with easterly winds that carry mineral dust from West Asia, which explains some of the positive aerosol anomalies during this period. As most of the long-distance dust transport occurs above the boundary layer (Dentener et al., 2010), these aerosol anomalies do not necessarily represent ground-level $PM_{2.5}$ trends.

O_3 concentrations followed a pattern similar to that of the AOD. The lockdown impact on NO_2, which has an atmospheric lifetime of approximately one day, is discernible locally, whereas O_3, which has a lifetime of days-weeks, is affected by long-distance transport associated with specific weather patterns. The tropospheric O_3changes determined in this study are similar to previous study results that reported a gradual O_3 decrease in the USA, Canada, Russia, and Europe (Talukdar et al., 2020); while in the month of May 2020 we also noted subtle increase in O_3 as observed by other study (Wu et al., 2020). Furthermore, the O_3 photochemistry in temperate latitudes from February–March is slower due to low solar irradiation, whereas at lower latitudes, O_3 buildup can be significant. Our findings showed a unique pattern of tropospheric pollutants over a longer period. The continuation of this trend in the future and its extent depends on the implementation of anthropogenic activity restrictions, which are primarily dictated by government policies.

An LST analysis was also performed to assess the impact of pollution on emitted radiation; however, LST is indirectly related to the radiation received by the earth's surface, which varies seasonally. The LST analysis results showed that the LST was decreased in Brazil, India, and Spain from January–May 2020 compared to the corresponding period of 2019. However, France, Germany, and the UK only showed a decreased average LST in February and March, which might be the impetus of the lockdown. No significant pattern was observed in the rest of the countries studied. Except for the LST reductions in the above-mentioned countries, the inconsistent LST patterns and changes are attributed to the seasonal shift of the Intertropical Convergence Zone caused by the location of the sun in the remaining investigated countries located in tropical, temperate, or sub-polar climate zones. Few studies have examined the relationship between LST and air pollution (Maithani et al., 2020; Song et al., 2018; Zheng et al., 2016; Feizizadeh and Blaschke, 2013); therefore, we performed this analysis as part of this study. The results showed that air pollution improvement has certain impacts on LST, which was evidenced in some countries by a declining LST trend throughout the study period, and in a few countries, it reduced immediately after the lockdown period began. A similar approach was utilized in a study conducted in India that highlighted the effect of the lockdown on the spatiotemporal LST patterns (Maithani et al., 2020). That study found that pollution levels were considerably lower during the lockdown period due to restricted vehicular movement and the absence of commercial and industrial activities, which caused a reduction in the greenhouse effect, allowing long-wave radiation to escape; therefore, the mean LSTs were lower in 2020 than in the previous years (Maithani et al., 2020). Another study performed a five-year (2001–2006) LST and $PM_{2.5}$ analysis that showed a concurrent increase in LST with $PM_{2.5}$, which could be attributed to the greenhouse effect of aerosol pollutants (Song et al., 2018). Another study conducted in Guangzhou, China, determined a strong correlation ($R^2 = 0.8$) between LST and $PM_{2.5}$ concentration, which generally fluctuates seasonally (Zheng et al., 2016). Feizizadeh and Blaschke found a correlation between highly air-polluted areas and LST in Tabriz and Iran, suggesting a direct impact of PM levels on LST (Feizizadeh and Blaschke, 2013). The findings in this study clearly show that AP levels decreased during the lockdown, which directly contributed to LST reductions.

Our analysis of more than 40 cities worldwide showed that the ground air pollution levels improved in most of the locations in 2020, albeit to a varying level, and is likely attributed to the restriction of anthropogenic activities during the lockdowns. The reductions in ground-level NO_2, $PM_{2.5}$, PM_{10}, and O_3 concentrations were evident in most studied locations (Shrestha et al., 2020). Asian (Delhi, Mumbai, Kolkata, Dhaka, Wuhan, Beijing, Istanbul, and Dubai) and European (Milan, Rome, Madrid, Berlin, and Paris) cities benefited the most from the lockdowns. Shrestha et al. performed a pollutant analysis of 40 cities worldwide from February 2019–March 2020 and determined that the pollution levels declined in most cities (Shrestha et al., 2020). This agrees with the findings of this study; however, our analysis of the lockdown reliably demonstrates both immediate and long-term impacts on pollutants and demarcates the differences between pollutants over a five-month period. Several recent short-term (one week or month duration) studies on the impact of the lockdowns on APs, however, insufficiently portray the actual impacts due to their short durations (Shrestha et al., 2020; Urrego and Urrego, 2020). Because the imposed lockdown dates, durations, and phases varied in the different countries, a long-term AP study should be performed. For example, in India, a complete lockdown was instituted at the end of March, whereas cities in western countries such as the USA, the UK, and South America observed multi-phase, partial lockdowns. Under such conditions, short-term studies on lockdown effects show its immediate impact on APs but do not show the concentration variations of the different pollutants in the different phases of unlocking the shutdown.

Biological studies have suggested that long- and short-term exposure to ambient ground-level O_3 and NO_2 can play an important role in the clinical manifestation of cardiorespiratory diseases (Conticini et al., 2020; Ogen, 2020; Travaglio et al., 2020; Lippi et al., 2020) and adversely affect organs targeted by SARS-CoV-2 (Brauer, 2010). Multiple studies have shown a relationship between APs and COVID-19 cases/mortalities in specific regions (Conticini et al., 2020; Cole et al., 2020; Qin et al., 2020; Wu et al., 2020); however, a global investigation of the long-term impact of APs on COVID-19 cases/mortalities is necessary. This study performed a comprehensive association analysis in locations with the worst virus outbreaks during the study period. The relationship between APs and COVID-19 has been studied; however, minimal studies have determined the role of specific APs in augmenting COVID-19 cases and deaths (Cole et al., 2020; Wu et al., 2020; Setti et al., 2020; Naqvi et al., 2021). Cole et al. examined long-term air pollution exposure in 355 Dutch municipalities to identify the relationship between $PM_{2.5}$, NO_2, and SO_2 concentrations with COVID-19 cases, hospital admissions, and deaths. The results showed a weak positive correlation between $PM_{2.5}$ and COVID-19 deaths ($R^2 = 0.23$) compared to the correlations with COVID-19 cases and hospital admissions ($R^2<0.15$) (Cole et al., 2020). The COVID-19 association with NO_2 and SO_2 concentrations was comparatively weaker ($R^2<0.1$) than that of $PM_{2.5}$. According to their model, the results revealed that a 1 $\mu g/m^3$ increase in the $PM_{2.5}$ concentration caused a 9.4%–15.1% increase in COVID-19 cases (Cole et al., 2020). Another study examined COVID-19 deaths in more than 3000 counties in the USA and reported that a 1 $\mu g/m^3$ increase in the $PM_{2.5}$ concentration caused an 8% increase in COVID-19 deaths. Therefore, a small increase in long-term $PM_{2.5}$ exposure can lead to a substantial increase in COVID-19 deaths (Wu et al., 2020). A high PM_{10} concentration was determined to be a significant predictor of COVID-19 infection in Italy (Setti et al., 2020). This study determined that northern Italian provinces with high PM_{10} concentrations had a median of 0.26 COVID-19 infections per 1000 residents, whereas southern Italian provinces with low PM_{10} concentrations had a median of 0.03 COVID-19 infections per 1000 residents (Setti et al., 2020). In this study, the major hotspots in India demonstrated a moderate positive correlation between COVID-19 mortalities (assessed at two time points) with the ground-level PM_{10} concentration ($R^2 = 0.145$; $r = 0.38$) and air quality index ($R^2 = 0.17$; $r = 0.412$) pollutant indicators (Naqvi et al., 2021). Overall, this study comprehensively analyzed tropospheric and ground-level APs and identified moderate positive association between ground-level NO_2 concentration and COVID-19 cases ($R^2 = 0.33$; $r = 0.57$) and mortalities ($R^2 = 0.40$; $r = 0.63$) and determined that NO_2 concentration is a reliable indicator. The weak-moderate positive relationship of O_3 pollutant was found with COVID-19 cases ($R^2 = 0.22$; $r = 0.47$) and mortalities ($R^2 = 0.12$; $r =$

0.35). However, no associations were observed between $PM_{2.5}$ and PM_{10} concentrations with COVID-19 cases and mortalities. We also performed analysis with all the data points included. Among the pollutants examined, NO_2 and O_3 showed weak correlation before outlier removal and this changed to moderate correlation after exclusion of outliers. For other pollutants ($PM_{2.5}$, and PM_{10}), negligible improvement in correlation was observed after removal of outliers.

We acknowledge few limitations of this study. **(i)** *Inconsistent lockdown period and stringency*: The study period assessed tropospheric and ground-level pollutant concentrations pre- and post-lockdown. However, the lockdown period was not the same for all the studied countries. Even within the same country, varied lockdown levels (full or partial) were imposed in different regions at different times. As such, a similar study period for pre- and post-lockdown for all the countries included in this study would have provided a more controlled analysis. The extent of lockdown period, stringency of lockdown, community social distancing and safety precautions influence viral spread that varied globally and is beyond the scope of the current study. **(ii)** *Data Availability*: Insufficient ground-level air quality indices and COVID-19 cases/mortality data for all cities have hindered extensive global analysis. **(iii)** *Percent change in air pollutants and its impact on correlation analysis of COVID-19 cases and mortality*. This study employed average monthly changes in air pollutants for correlation with COVID-19 cases and mortality; however, we did not account for the lag times due to the SARS-CoV-2 incubation period (generally considered as 15 days). This may have yielded different results outcomes. **(iv)** We did not normalize our data with other confounders such as the population density, proportion of ageing population and social distancing implementation. Even with the aforementioned limitations, this study mainly focused on assessing global air pollution improvement due to the lockdowns. Correlating the clinical outcomes of COVID-19 with adverse air pollution conditions would support the findings of this study and will provide a roadmap for research on the effect of APs on future pandemics related to chronic respiratory diseases. This would facilitate the development of public health policies to prepare for pandemics and mitigate their adverse effects in polluted, densely populated regions worldwide.

Declaration of competing interest

The authors declare that they have no known competing financial interests or personal relationships that could have appeared to influence the work reported in this paper.

Appendix A. Supplementary data

Supplementary data to this article can be found online at https://doi.org/10.1016/j.apr.2021.101172.

Data and materials availability

All data required to evaluate the conclusions in this study are presented in the manuscript and Supplementary Materials.

Author statement

Hasan Raja Naqvi: Conceptualization, Methodology, Validation, Formal analysis, Investigation, Resources, Writing – original draft, Reviewing and Editing. Guneet Mutreja: Methodology, Validation, Formal analysis, Resources. Mohammad Hashim: Methodology, Validation, Formal analysis, Resources. Abhra Singh: Methodology, Validation, Formal analysis, Resources. Md Nawazuzzoha: Methodology, Validation, Formal analysis, Resources. Darakhsha Fatima Naqvi: Methodology, Validation, Formal analysis, Resources. Adnan Shakeel: Methodology, Formal analysis, Resources. Masood Ahsan Siddiqui: Resources, Writing- Reviewing and Editing. Anis Ahmad Chaudhary: Methodology, Writing- Reviewing and Editing of Revised Manuscript. Afsar Naqvi: Conceptualization, Investigation, Resources, Writing – original draft, Reviewing and Editing.

References

Biswal, A., et al., 2020. COVID-19 lockdown and its impact on tropospheric NO2 concentrations over India using satellite-based data. Heliyon6, e04764. https://doi.org/10.1016/j.heliyon.2020.e04764.

Brauer, M., 2010. How much, how long, what, and where: air pollution exposure assessment for epidemiologic studies of respiratory disease. Proc. Am. Thorac. Soc. 7, 111–115. https://doi.org/10.1513/pats.200908-093rm.

Cole, M.A., Ozgen, C., Strobl, E., 2020. Air Pollution Exposure and COVID-19. DISCUSSION PAPER SERIESIZA DP No. 13367. IZA – Institute of Labor Economics. http://ftp.iza.org/dp13367.pdf.

Conticini, E., Frediani, B., Caro, D., 2020. Can atmospheric pollution be considered a co-factor in extremely high level of SARS-CoV-2 lethality in Northern Italy?*. Environ. Pollut. 261, 114465.

Coronavirus COVID-19 Live Tracker Johns Hopkins. https://www.grainmart.in/news/coronavirus-covd-19-live-cases-tracker-john-hopkins/.

Cucinotta, D., Vanelli, M., 2020. WHO declares COVID-19 a pandemic. Acta Biomed. 91, 157–160. https://doi.org/10.23750/abm.v91i1.9397.

Dentener, F., Keating, T., Akimoto, H., 2010. Convention on Long-Range Transboundary Air Pollution, United Nations, Hemispheric Transport of Air Pollution 2010: Part A-Ozone and Particulate Matter (UN, 2010).

Dutheil, F., Baker, J.S., Navel, V., 2020. COVID-19 as a factor influencing air pollution? Environ. Pollut. 263, 114466. https://doi.org/10.1016/j.envpol.2020.114466.

ESA (European Space Agency), 2020. https://www.esa.int/Applications/Observing_the_Earth/Copernicus/Sentinel-5P.

Fan, C., et al., 2020. The impact of the control measures during the COVID-19 outbreak on air pollution in China. Rem. Sens. 12, 1613.

Feizizadeh, B., Blaschke, T., 2013. Examining urban heat island relations to land use and air pollution: multiple end member spectral mixture analysis for thermal remote sensing. IEEE Journal of Selected Topics in Applied Earth Observations and Remote Sensing 6, 1749–1756. https://doi.org/10.1109/jstars.2013.2263425.

Freychet, N., Tett, S.F.B., Bollasina, M., Wang, K.C., Hegerl, G.C., 2019. The local aerosol emission effect on surface shortwave radiation and temperatures. J. Adv. Model. Earth Syst. 806–817. https://doi.org/10.1029/2018MS001530.

Fu, F., Purvis-Roberts, K.L., Williams, B., 2020. Impact of the COVID-19 pandemic lockdown on air pollution in 20 major cities around the world. Atmosphere 11, 1189. https://doi.org/10.3390/atmos11111189.

Gautam, S., 2020. COVID-19: air pollution remains low as people stay at home. Air Quality, Atmosphere & Health13 853–857. https://doi.org/10.1007/s11869-020-00842-6.

Gorelick, N., et al., 2017. Google earth engine: planetary-scale geospatial analysis for everyone. Remote Sens. Environ. 202, 18–27.

Hashim, B.M., Al-Naseri, S.K., Al-Maliki, A., Al-Ansari, N., 2021. Impact of COVID-19 lockdown on NO_2, O_3, $PM_{2.5}$ and PM_{10} concentrations and assessing air quality changes in Baghdad, Iraq. Sci. Total Environ. 754, 141978.

Huang, C., et al., 2020. Clinical features of patients infected with 2019 novel coronavirus in Wuhan, China. Lancet 395, 497–506. https://doi.org/10.1016/S0140-6736(20)30183-5.

Huang, Y., Dickinson, R.E., Chameides, W.L., 2006. Impact of aerosol indirect effect on surface temperature over East Asia. Proc. Natl. Acad. Sci. Unit. States Am. 4371–4376. https://doi.org/10.1073/pnas.0504428103.

Jin, M., Shepherd, M., Zheng, W., 2010. Urban surface temperature reduction via the urban aerosol direct effect: a remote sensing and wrf model sensitivity study. Advances in Meteorology 1–14. https://doi.org/10.1155/2010/681587.

Konstantinoudis, G., Padellini, T., Bennett, J.E., Davies, B., Ezzati, M., Blangiardo, M., 2020. Long-term exposure to air-pollution and COVID-19 mortality in England: a hierarchical spatial analysis. Public Glob Health 146, 106316. https://doi.org/10.1101/2020.08.10.20171421.

Kumari, P., Toshniwal, D., 2020. Impact of lockdown on air quality over major cities across the globe during COVID-19 pandemic. Urban climate 34, 100719. https://doi.org/10.1016/j.uclim.2020.100719.

Leibniz Institute for Tropospheric Research (TROPOS), 2020. Traffic density, wind and air stratification influence concentrations of air pollutant NO2: leipzig researchers use a calculation method to remove weather influences from air pollution data. Science Daily, 26 June 2020. www.sciencedaily.com/releases/2020/06/200626114750.htm.

Lippi, G., Sanchis-Gomar, F., Henry, B.M., 2020. Association between Environmental Pollution and Prevalence of Coronavirus Disease 2019 (COVID-19) in Italy. medRxiv pre-print. https://doi.org/10.1101/2020.04.22.20075986.

Liu, F., Wang, M., Zheng, M., 2021. Effects of COVID-19 lockdown on global air quality and health. Sci. Total Environ. 755, 142533. https://doi.org/10.1016/j.scitotenv.2020.142533.

Maithani, S., Nautiyal, G., Sharma, A., 2020. Investigating the effect of lockdown during COVID-19 on land surface temperature: study of dehradun city, India. J Indian Soc Remote Sens 48, 1297–1311. https://doi.org/10.1007/s12524-020-01157-w.

Mele, M., Magazzino, C., 2020. Pollution, economic growth, and COVID-19 deaths in India: a machine learning evidence. Environ. Sci. Pollut. Res. 28, 2669–2677. https://doi.org/10.1007/s11356-020-10689-0.

Menut, L., 2020. Impact of lockdown measures to combat Covid-19 on air quality over Western Europe. Sci. Total Environ. 140426. https://doi.org/10.1016/j.scitotenv.2020.140426.

Nakada, L.Y.K., Urban, R.C., 2020. COVID-19 Pandemic: Impacts on the Air Quality during the Partial Lockdown in Sao Paulo. Science of The Total Environment730, Brazil, p. 139087. https://doi.org/10.1016/j.scitotenv.2020.139087.
Naqvi, H.R., et al., 2020. Improved air quality and associated mortalities in India under COVID-19 lockdown. Environ. Pollut. 268, 115691. https://doi.org/10.1016/j.envpol.2020.115691.
Naqvi, H.R., Mutreja, G., Shakeel, A., Siddiqui, M.A., 2021. Spatio-temporal analysis of air quality and its relationship with major COVID-19 hotspot places in India. Remote Sensing Applications: Society and Environment 22, 100473. https://doi.org/10.1016/j.rsase.2021.100473.
NASA, 2020. Airborne Nitrogen Dioxide Plummets over China. https://earthobservatory.nasa.gov/images/146362/airborne-nitrogen-dioxide-plummets-over-china.
Ogen, Y., 2020. Assessing nitrogen dioxide (NO2) levels as a contributing factor to corona-virus (COVID-19) fatality. Sci. Total Environ. 726, 138605, 2020.
Pansini, R., Fornacca, D., 2020. Higher virulence of COVID-19 in the air polluted regions of eight severely affected countries. Epidemiology. https://doi.org/10.1101/2020.04.30.20086496.
Qin, C., Zhou, L., Hu, Z., et al., 2020. Dysregulation of immune response in patients with COVID-19 in Wuhan, China. Clin. Infect. Dis. 71, 762–768. https://doi.org/10.1093/cid/ciaa248.
Ratner, B., 2009. The correlation coefficient: its values range between +1/−1, or do they? J. Target Meas. Anal. Market. 17, 139–142. https://doi.org/10.1057/jt.2009.5.
Schraufnagel, D.E., et al., 2019. Air pollution and non-communicable diseases: a review by the forum of international respiratory societies' environmental committee, Part 2: air pollution and organ systems. Chest 155, 417–426. https://doi.org/10.1016/j.chest.2018.10.041.
Setti, L., et al., 2020. Airborne transmission route of COVID-19: why 2 meters/6 feet of inter-personal distance could not Be enough. Int. J. Environ. Res. Publ. Health 17, 2932. https://doi.org/10.3390/ijerph17082932.e.
Shrestha, A.M., et al., 2020. Lockdown Caused by COVID-19 Pandemic Reduces Air Pollution in Cities Worldwide. Pre-print. Earth ArXiv. https://doi.org/10.31223/osf.io/edt4j.
Sicard, P., et al., 2020. Amplified ozone pollution in cities during the COVID-19 lockdown. Sci. Total Environ. 139542. https://doi.org/10.1016/j.scitotenv.2020.139542.
Singh, R.P., Chauhan, A., 2020. Impact of lockdown on air quality in India during COVID-19 pandemic. Air Qual Atmos Health13. https://doi.org/10.1007/s11869-020-00863-1, 921–92.
Solimini, A., Filipponi, F., Fegatelli, D.A., et al., 2021. A global association between Covid-19 cases and airborne particulate matter at regional level. Sci. Rep. 11, 6256. https://doi.org/10.1038/s41598-021-85751-z.
Song, Z., et al., 2018. Global land surface temperature influenced by vegetation cover and $PM_{2.5}$ from 2001 to 2016. Rem. Sens. 10, 2034. https://doi.org/10.3390/rs10122034.
State of Global Air 2019, 2019. Health Effects Institute.
Steiner, A.L., Mermelstein, D., Cheng, S.J., Twine, T.E., Oliphant, A., 2013. Observed impact of atmospheric aerosols on the surface energy budget. (2013). Earth Interact. 1–22. https://doi.org/10.1175/2013EI000523.1.
Talukdar, S., et al., 2020. Modelling the Global Air Quality Conditions in Perspective of COVID-19 Stimulated Lockdown Periods Using Remote Sensing Data. Pre-print, Research Square. https://doi.org/10.21203/rs.3.rs-70252/v1.
Tobías, A., et al., 2020. Changes in air quality during the lockdown in Barcelona (Spain) one month into the SARS-CoV-2 epidemic. Sci. Total Environ. 726, 1–4.
Travaglio, M., Yu, Y., Popovic, R., Leal, N.S., Martins, L.M., 2020. Links between Air Pollutionand COVID-19 in England. MedRxiv, 2020.04.16.20067405.
Urrego, D.R., Urrego, L.R., 2020. Air quality during the COVID-19: PM2.5 analysis in the 50 most polluted capital cities in the world. Environ. Pollut. 115042. https://doi.org/10.1016/j.envpol.2020.115042.
USGS. https://lpdaac.usgs.gov/products/mcd19a2v006/.
Veefkind, J.P., et al., 2012. TROPOMI on the ESA Sentinel-5 Precursor: a GMES mission for global observations of the atmospheric composition for climate, air quality and ozone layer applications. Remote Sens. Environ. 120, 70–83.
Venter, Z.S., Aunan, K., Chowdhury, S., Lelieveld, J., 2020. COVID-19 lockdowns cause global air pollution declines. Proc. Natl. Acad. Sci. U. S. A. 117, 18984–18990. https://doi.org/10.1073/pnas.2006853117.
Viehmann, A., et al., 2015. Long-term residential exposure to urban air pollution, and repeated measures of systemic blood markers of inflammation and coagulation. Occup. Environ. Med. 72, 656–663. https://doi.org/10.1136/oemed-2014-102800.
Wan, Z., Hook, S., Hulley, G., 2015. MOD11A1 MODIS/Terra Land Surface Temperature/Emissivity Daily L3 Global 1km SIN Grid V006 [Data Set]. NASA EOSDIS Land Processes DAAC. https://doi.org/10.5067/MODIS/MOD11A1.006. Accessed on 2020-05-19.
Who, 2014. Burden of Disease from Household Air Pollution for 2012: Summary of Results.
Worldwide air quality monitoring data. https://aqicn.org/sources/.
Wu, X., et al., 2020. Exposure to Air Pollution and COVID-19 Mortality in the United States: A Nationwide Cross-Sectional Study. medRxiv pre-print. https://www.medrxiv.org/content/10.1101/2020.04.05.20054502v2.
Yao, Y., Pan, J., Liu, Z., Meng, X., Wang, W., Kan, H., et al., 2020. Temporal association between particulate matter pollution and case fatality rate of COVID-19 in Wuhan. Environ. Res. 189, 109941. https://doi.org/10.1016/j.envres.2020.109941.
Zheng, Z., Chen, Y., Wu, Z., Qian, Q., 2016. Correlation between land surface temperature inversion (based on Landsat-8) and $PM_{2.5}$ concentration: taking Guangzhou as an example. In: 4th International Workshop on Earth Observation and Remote Sensing Applications (EORSA).
Zhu, Y., Xie, J., Huang, F., Cao, L., 2020. Association between short-term exposure to air pollution and COVID-19 infection: evidence from China. Sci. Total Environ. 727, 138704. https://doi.org/10.1016/j.scitotenv.2020.138704.